Design Parameters for Sampled-Data Drives for CNC Machine Tools

YORAM KOREN, MEMBER, IEEE, AND JOHN G. BOLLINGER

Abstract—**A mathematical analysis of a typical sampled-data servo-drive for computer numerial control (CNC) machine tools is presented with the objective of providing the control engineer with useful design charts for the selection of system parameters. A mathematical model is first developed which facilitates the evaluation of the relation between servo-loop gain and computer sampling rate. The question of stability is reviewed, and a solution for the time response of the sampled-data system is presented. Different performance criteria are discussed including: selection of desired damping factor; maximum overshoot; integral of speed square-error; position steady-state error; and the absolute value of the error. The latter criterion has been chosen as the most useful approach. System performance evaluation is presented in the form of dimensionless charts. A final design procedure is recommended which utilizes a dimensionless chart to select sample rate and gain in order to achieve an optimal performance consistent with allowable contouring accuracy and closed-loop bandwidth.**

INTRODUCTION

A COMPUTER numerical control (CNC) system may utilize many alternative types of position control. One method wherein feedback is achieved with an external digital control loop is discussed and compared in [1]. Reference pulses generated by the mini-computer are supplied to the digital logic. This type of control uses an up-down counter as a comparator element, and was also discussed in [2] and [3]. An alternative control method uses the mini-computer as part of the control loop by replacing the up-down counter. The computer samples the feedback signal, compares it with the reference, and sends the resulting error through a digital-to-analog converter (DAC) to drive the motor. A block diagram of this system is presented in Fig. 1.

Although a digital encoder is used in the block diagram of Fig. 1, a resolver or an inductosyn could be used as the feedback device. The interface circuitry will differ depending on the hardware chosen. The interface to a digital encoder is the simplest. It consists of a buffered counter which is incremented by the pulses produced by the encoder. The mini-computer samples the contents of the counter at fixed time intervals and immediately clears it. The counter contents is subtracted from, or added to, a software up-down counter

Paper ID 75-03, approved by the Industrial Drives Committee of the IEEE Industry Applications Society for presentation at the 1975 Tenth Annual Meeting of the IEEE Industry Applications Society, Atlanta, GA, September 28–October 2. Manuscript released for publication November 29, 1977.

Y. Koren is with the Technion–Israel Institute of Technology, Haifa, Israel.

J. G. Bollinger is with the College of Engineering, University of Wisconsin, Madison, WI 53706.

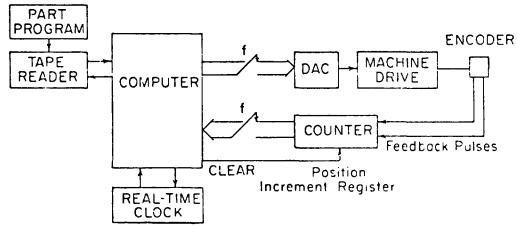

Fig. 1. Typical sampled-data servo-drive for CNC machine tool.

which serves as the loop's comparator. Notice that the output register of the computer with the DAC typically plays the role of a zero-order-hold (ZOH) circuit, which must be included in computing the transfer function for the entire drive.

THE PROBLEM OF DESIGN

The described system belongs to a class of real-time control systems in which the feedback signal is sampled at fixed intervals, processed in the computer, and returned via a DAC. Comparing such a system with its continuous counterparts, there is a main difference; namely, the signal fed to the machine drive is not a continuous signal, but a sampled-data reconstructed stepwise constant velocity reference.

A block diagram representation of the system under consideration is shown in Fig. 2. The counter associated with the encoder does not affect the system performance, and therefore is not noted in the figure. Actually, there are two samplers in the circuit; however, their location in the loop requires consideration of only one of them. In order to present the classical error-sampled control system, the error-sampler alone will be considered. The transfer function of the ZOH is well known where T is the sample time. The transfer function of the machine drive assumes the simplest model where τ is the mechanical time-constant of the motor. The open-loop gain of the system is

$$K = K_c K_m K_e \tag{1}$$

where

- K_c includes the gains of the DAC in [V/pulse] and the power amplifier;
- K_e is the encoder gain in [pulse/rad];
- K_m is measured in [rad/s/V].

Numerical solutions to particular examples of the system presented in Fig. 2 can be found in the literature: e.g., in [4,

0093-9994/78/0300-0255$00.75

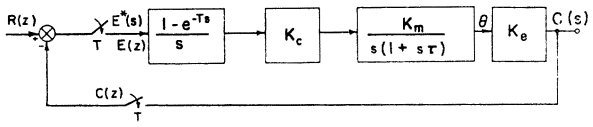

Fig. 2. Block diagram of control loop.

pp. 125-129]; [5, pp. 128-131 and pp. 173-175]; [6, pp. 139-140]; [7, pp. 145-149]. However, a general solution to the problem of this class of servo system design has not been presented in any of these sources.

A general mathematical solution to a system similar to the one in Fig. 2 but without the ZOH was presented in [8]. In [5, pp. 132-142] and [6, pp. 327-336], the maximum overshoot problem has been discussed, but again, a system which contains a ZOH can not be investigated using these methods since they assume only two dominant poles in the closed-loop transfer function.

The second-order sampled-data system was solved also in [7, pp. 170-178] where maximum overshoot and damping graphs have been obtained. However, in this reference a certain pole-zero configuration of the closed-loop transfer-function is assumed, rather than a system in which the pole-zero locations must be determined from the open-loop parameters. The latter is the approach treated in this paper.

STABILITY ANALYSIS

The open-loop transfer function is

$$G(s) = \frac{1 - e^{-sT}}{s} \cdot \frac{K}{s(1 + s\tau)}. \tag{2}$$

The first step in the analysis involves a determination of the open-loop z transform function $G(z)$. It can be found by a partial-fraction expansion of $G(s)$, and conversion, term by term, to z transforms with the aid of an appropriate table:

$$G(s) = K[1 - e^{-sT}] \left(\frac{1}{s^2} - \frac{\tau}{s} + \frac{\tau}{s + 1/\tau} \right). \tag{3}$$

After z transformation

$$G(z) = K \left(\frac{z - 1}{z} \right) \left[\frac{Tz}{(z-1)^2} - \frac{\tau z}{z - 1} + \frac{\tau z}{z - e^{-T/\tau}} \right]. \tag{4}$$

For simplicity, the term $e^{-T/\tau}$ will be defined henceforth as E. From (4)

$$G(z) = \frac{(z - E)[T - \tau(z - 1)] + \tau(z - 1)^2}{(z - 1)(z - E)} K. \tag{5}$$

For stability analysis the polynomial of interest is the numerator of $1 + G(z)$, denoted as $P(z)$:

$$P(z) = z^2 + z\{K[T - \tau(1 - E)] - (1 + E)\} + K[\tau(1 - E) - TE] + E. \tag{6}$$

The closed-loop system is stable if $P(z)$ possesses no zeros outside the unit circle in the z plane. In the general case, the determination of whether there is a zero outside this circle involves extensive effort, but since the polynomial in (6) is a quadratic and has real coefficients, the necessary and sufficient conditions for $P(z)$ to have no zeros outside the unit circle are [9]

$$|P(0)| < 1 \qquad P(1) > 0 \qquad P(-1) > 0.$$

These three conditions lead to the following relations:

$$K[\tau - E(T + \tau)] + E < 1 \tag{7-1}$$

$$KT(1 - E) > 0 \tag{7-2}$$

$$2 + 2E + K[2\tau(1 - E) - T(1 + E)] > 0. \tag{7-3}$$

The second condition is satisfied for any positive K, but the first and third conditions place a bound on the gain. They can be rewritten in the following form:

$$K\tau < \frac{1 - E}{1 - E - (T/\tau)E} \tag{8}$$

$$K\tau < \frac{2(1 + E)}{(T/\tau)(1 + E) - 2(1 - E)}. \tag{9}$$

It is worthwhile to notice that the equivalent continuous system is always stable. The two boundaries have an intersection point at

$$\frac{T}{\tau} = \frac{4(1 - E)}{1 + E}. \tag{10}$$

Recalling that E was defined as $E = e^{-T/\tau}$, the intersection point was calculated to be at $T/\tau = 3.830$. Therefore, as long as T/τ ranges from 0 through 3.83, the stability boundary is given by (8). This boundary is shown in Fig. 3. (The curve which is corresponded to $\xi = 0$.)

Usually τ is measured in seconds and K in 1/s. But the practice in NC systems is to present K in units of in/min/mil. Obviously, a K which is given in 1/s must be divided by 50/3 to convert its units to in/min/mil.

TIME RESPONSE

The transfer function of the closed-loop as determined from (5) yields

$$\frac{C(z)}{R(z)} = \frac{G(z)}{1 + G(z)} = \frac{Az + B}{z^2 + z(A - 1 - E) + B + E} \tag{11}$$

where

$$A = K[T - \tau(1 - E)]$$
$$B = K[\tau(1 - E) - TE]. \tag{11a}$$

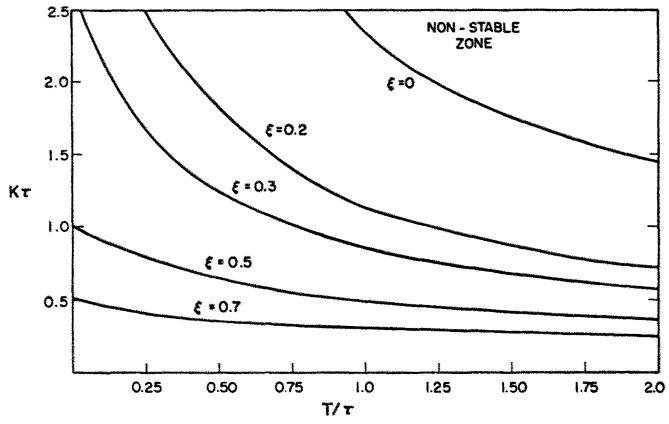

Fig. 3. Gain versus sampling period for constant damping factors.

When a unit step is applied to the input, the output transform is given by

$$C(z) = \frac{Az + B}{z^2 - z(1 + E - A) + B + E} \cdot \frac{z}{(z-1)}. \tag{12}$$

Equation (12) can be rearranged to

$$C(z) = \frac{z}{z-1} - \frac{z\left(z - \dfrac{1+E-A}{2}\right) + z\dfrac{1-E-A}{2}}{z^2 - z(1+E-A) + B + E}. \tag{13}$$

Thus

$$C(z) = \frac{z}{z-1} - \frac{z(z - a\cos\omega T) + zaM\sin\omega T}{z^2 - 2za\cos\omega T + a^2} \tag{14}$$

where

$$a^2 = B + E \tag{15}$$

$$\cos\omega T = (1 + E - A)/2a \tag{16}$$

$$\sin\omega T = \pm\frac{1}{2a}\sqrt{4a^2 - (1+E-A)^2}$$

$$= \pm\frac{(1-E)}{2a}\sqrt{4K\tau - (1-D)^2} \tag{17}$$

$$D = A/(1-E) \tag{18}$$

$$M = \frac{1-E-A}{2a\sin\omega T} = \frac{1-D}{\pm\sqrt{4K\tau - (1-D)^2}}$$

$$= \frac{\gamma}{\pm\sqrt{1-\gamma^2}} \tag{19}$$

$$\gamma = (1-D)/2\sqrt{K\tau}.$$

The plus sign is used in (17) and (19) for $0 < \omega T < \pi$, while for $\pi \leqslant \omega T < 2\pi$, the minus sign is used.

The time response is obtained by applying the z transform tables on (14):

$$C_n = 1 - e^{-\alpha nT}(\cos\omega nT + M\sin\omega nT) \tag{20}$$

where

$$e^{-\alpha nT} = a^n. \tag{21}$$

C_n describes the output at the sampling instants nT: α and ω are proportional to the damping and the frequency of the response. The value of α is determined from (15) and (21) which yield

$$\alpha = -\frac{1}{T}\ln(a) = -\frac{1}{2T}\ln\left[E\left(1 - KT + K\tau\frac{1-E}{E}\right)\right]$$

$$= \frac{1}{2\tau} - \frac{1}{2T}\ln\left(1 - KT + K\tau\frac{1-E}{E}\right). \tag{22}$$

Notice that $\alpha = 0$ prescribes a stability condition, which in turn is identical to the one in (8). The value of ω can be determined from (16) and (17):

$$\omega = \omega_0 + n\pi/T \tag{23}$$

where

$$\omega_0 = \frac{1}{T}\tan^{-1}\frac{\sqrt{4K\tau - (1-D)^2}}{\dfrac{1+E}{1-E} - D} \tag{24}$$

and

$$n = 0, \qquad \text{for } 0 \leqslant \omega_0 T < \pi/2$$

$$n = 1, \qquad \text{for } \pi/2 \leqslant \omega_0 T < 3\pi/2.$$

To compare the sampled-data solution with the well-known continuous case response, one must substitute the following in (18)-(24):

$$T \to 0; \qquad 1 - E = T/\tau; \qquad E = 1$$

In this case the values of A and D are zero, and

$$\alpha = 1/2\tau = \xi\omega_n \tag{25}$$

where ξ is denoted as the damping factor and ω_n is the natural frequency defined as $\sqrt{K/\tau}$;

$$\gamma = 1/2\sqrt{K\tau} = \xi \tag{26}$$

$$M = \xi/\sqrt{1-\xi^2} \tag{27}$$

$$\omega = \frac{1}{T}\tan^{-1}\frac{T\sqrt{1-\xi^2}\omega_n}{\xi} = \sqrt{1-\xi^2}\omega_n. \tag{28}$$

DRIVE PERFORMANCE CRITERIA

Determining the stability of a sampled-data machine tool drive is not sufficient. It is necessary to ascertain the degree of stability as well as accuracy, and following error, etc. In general, to obtain information one must settle on an acceptable performance criteria for the system. Five specific criteria were chosen for this investigation and will be presented here, including:

a) the damping factor,
b) the maximum overshoot to a step speed command,
c) the integral of the speed square-error,
d) the steady-state following error,
e) the integral of the absolute-error.

In order to achieve generalization of the curves, the results are plotted on a dimensionless plane of $K\tau$ versus T/τ.

The Damping Factor

To define a damping factor in the sampled-data system, consider the equivalent definition in the continuous case. From (25) and (28),

$$\alpha = \frac{\xi\omega}{\sqrt{1-\xi^2}} \tag{29}$$

or

$$\xi = \frac{\alpha}{\sqrt{\alpha^2+\omega^2}} = \frac{\alpha T}{\sqrt{(\alpha T)^2+(\omega T)^2}}. \tag{30}$$

Equation (30) defines the damping factor of the sampled-data system, where α and ω are given in (22), (23), and (24). The curves which were obtained for various values of ξ are shown in Fig. 3. Obviously, the plot for $\xi = 0$ is identical with the one obtained from (8).

Maximum Overshoot

In sampled-data systems the maximum overshoot cannot be determined from a discrete-time equation, such as (20) since the maximum overshoot may not occur exactly at a sampling instant. Therefore the determination of the maximum overshoot is performed by using the continuous system response equation for a unit step input

$$c(t) = 1 - e^{-\alpha t}(\cos \omega t + M \sin \omega t). \tag{31}$$

Obviously $c(t)$ passes through the points of c_n. The corresponding continuous error is

$$e(t) = e^{-\alpha t}(\cos \omega t + M \sin \omega t). \tag{32}$$

The maximum error is determined by taking the first derivative of $e(t)$ with respect to time and equating it to zero. This yields

$$\tan(\omega t - n\pi) = \frac{\omega M - \alpha}{\alpha M + \omega}.$$

The maximum is obtained for $n = 1$, and the corresponding time t is denoted as t_{max}:

$$t_{max} = \frac{1}{\omega}\left(\pi + \tan^{-1}\frac{\omega M - \alpha}{\alpha M + \omega}\right). \tag{33}$$

The maximum error can be computed by substituting t_{max} into (32) which yields

$$e_{max} = -\omega\sqrt{\frac{1+M^2}{\alpha^2+\omega^2}}\, e^{-\alpha t_{max}}. \tag{34}$$

Some results of $-e_{max}$ are shown in Fig. 4. Notice that the maximum overshoot can exceed 100 percent and the system is still stable.

The Integral of the Square Error

The performance criterion under consideration in this section is

$$p = \frac{1}{\tau}\int_0^\infty e^2(t)\,dt. \tag{35}$$

Substituting of (32) into (35) and integrating yields

$$p = \frac{T/\tau}{4\alpha T}\left[1 + \frac{(M\omega T + \alpha T)^2}{(\alpha T)^2 + (\omega T)^2}\right]. \tag{36}$$

αT and ωT are given by (22), (23), and (24). Loci of constant p have been computed, and the results are shown in Fig. 5. The most interesting result is that an optimal point exists for every value of T/τ. The locus of these optimal points is plotted as the optimal curve in Fig. 5.

It is worthwhile to notice that the optimal loci shown in Fig. 5 present a new design concept which is applicable only to sampled-data systems. In a second-order continuous system the equivalent criteria is

$$\min\left\{\int_0^\infty e^2(t)\,dt\right\} = \min\left\{\frac{1+4\xi^2}{4\xi\omega_n}\right\} \tag{37}$$

which gives a minimum for $\xi = 0.5$. Notice that in this solution ω_n is treated as a constant, which means that the ratio K/τ must be constant. On the other hand, when determining the optimal loci of Fig. 5 for the sampled-data system, no limitations were imposed on the system.

In order to apply the criterion prescribed by (37), we have to define an ω_n for a sampled-data system. By comparing (25) and (30), an ω_n can be defined as follows:

$$\omega_n = \sqrt{\alpha^2+\omega^2}. \tag{38}$$

The new criterion will be

$$\min\left\{\omega_n\int_0^\infty e^2(t)\,dt\right\} = \min\{\tau\omega_n p\}. \tag{39}$$

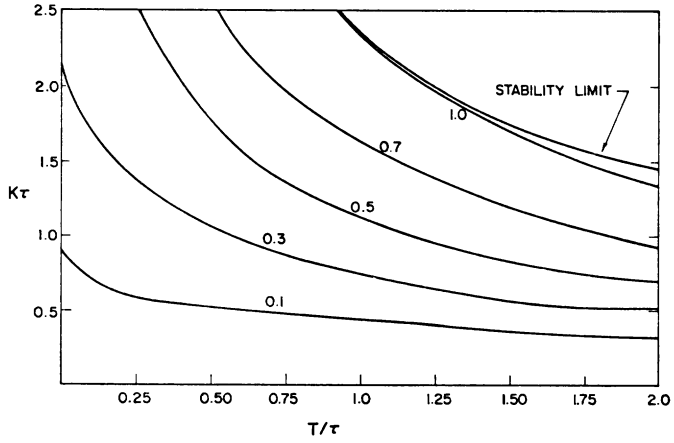

Fig. 4. Gain versus sampling period with maximum overshoot error as parameter.

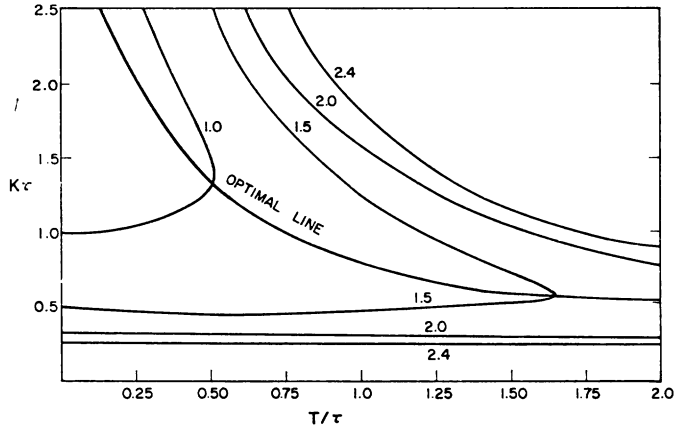

Fig. 5. Loci of square-error integral (no limits on system).

The value of $\tau\omega_n p$ is calculated from (36), (25), and (38):

$$\tau\omega_n p = \frac{1}{4\xi}\left[1 + \left(\frac{M\omega}{\omega_n} + \xi\right)^2\right]. \tag{40}$$

The optimal ξ which results in a minimum of $(\tau\omega_n p)$ was computed, and it has been found that the optimal ξ is very close to its continuous case value of 0.5. The locus corresponding with the optimal ξ was plotted in Fig. 6. The parameter in Fig. 6 is $\tau\omega_n p$.

When comparing with Fig. 3, the optimal locus lies slightly above the line of $\xi = 0.5$. This locus provides a very useful tool for a designer who prefers the integral of the square error as the significant criterion. The value of the minimal T, or T/τ, is usually prescribed by the processing time of the CNC program. Once T is known, the value of K may be determined by using the optimal line in Fig. 6. For example, in a system in which both the time-constant and the sampling period are 10 ms, the optimal K is 54 s^{-1}, or 3.24 in/min/mil, and the corresponding damping factor is $\xi = 0.487$.

Steady-State Error

In NC systems the most common input to the described control loop is a ramp. This input is typical in linear interpolation and point-to-point operation. (For circular interpolation a sine input is provided.) For this study, a unity slope ramp will be used as the input. When a unit ramp is applied, (20) and (31) describe the speed of the motor (multiplied by K_e), while (32) describes the speed error, which is of course zero in the steady state. Similarly, the error discussed in the latter two sections above is the speed error, multiplied by K_e. Another significant criterion in such a system is the position error ϵ, which is determined by integrating (32):

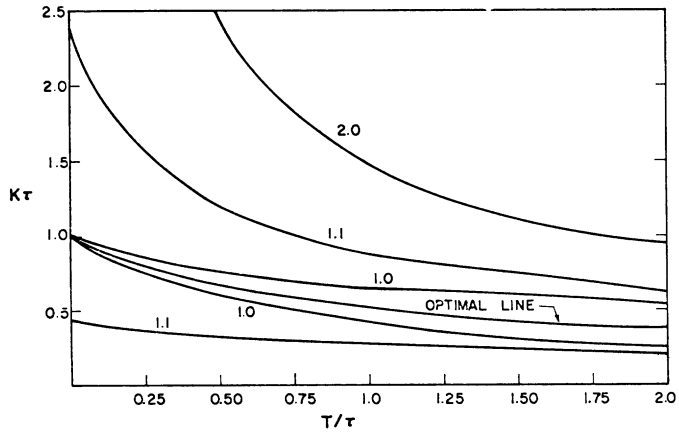

Fig. 6. Loci of square-error integral with $\tau\omega_n p$ as patameter and optimal line corresponding with optimal ξ.

$$\epsilon = \frac{\alpha + M\omega}{\alpha^2 + \omega^2} + \frac{e^{-\alpha t}}{\alpha^2 + \omega^2}[(\omega - M\alpha)\sin\omega t - (\alpha + M\omega)\cos\omega t]. \tag{41}$$

The steady-state position error contains the first term only. Since our discussion involves a dimensionless coordinate system, the criterion under consideration will be

$$E_s = \frac{1}{\tau}\int_0^\infty e(t)\,dt = \left(\frac{T}{\tau}\right)\frac{\alpha T + M\omega T}{(\alpha T)^2 + (\omega T)^2}. \tag{42}$$

As it is well known in the equivalent continuous system

$$\tau E_s = \frac{1}{K}, \tag{43}$$

which means that a zero steady-state error cannot be achieved in a continuous type 1 servo-system. Fig. 7 shows contours for constant values of steady state error E_s. Notice that the position steady-state error decreases with increasing T. Also, the value of E_s decreases for increasing $K\tau$. Thus a zero steady-state error can be obtained in the sampled-data system. However, working on the zero-error curve is not practical, since in this case the system is too close to the unstable zone and the system is hunting.

The Integral of the Absolute Error

Minimizing the integral of the square error, essentially infers an attempt to cut down the large servo errors at the cost of many small errors. When applying a step function, the maximum error occurs just after applying the step. The square

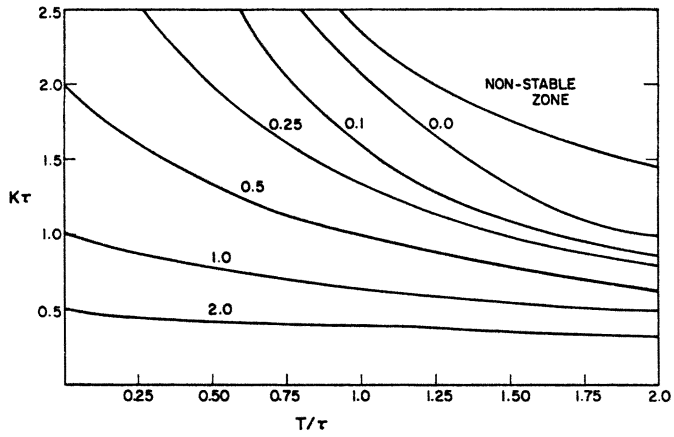

Fig. 7. Gain versus sampling period for constant steady-state errors.

error criterion emphasizes this large error, and consequently causes a rapid increase of the output. The result is a system with a relatively large overshoot. Therefore, it is worthwhile to consider carefully the worthiness of such a design criterion in feedback control systems. A better criterion might be one in which any error has the same weight, or in other words, minimizing the integral of the absolute error, I.

The error $e(t)$ is given in (32). The error is zero at times t_n, where t_n is the crossing time. Thus the criterion I can be written as

$$I = \int_0^\infty |e(t)|\,dt = \int_0^{t_1} e(t)\,dt - \int_{t_1}^{t_2} e(t)\,dt + \int_{t_2}^{t_3} e(t)\,dt - \int_{t_3}^{t_4} e(t)\,dt + \cdots. \tag{44}$$

Defining

$$\int_{t_{n-1}}^{t_n} e(t)\,dt = E(t_n) - E(t_{n-1}), \tag{45}$$

(44) can be written as

$$I = -E(0) + 2[E(t_1) - E(t_2) + E(t_3) \cdots]. \tag{46}$$

Values of $E(t_n)$ can be obtained by using (41):

$$E(t_n) = E_n = F_n e^{-\alpha t_n} \tag{47}$$

where

$$F_n = \frac{1}{\alpha^2 + \omega^2}[(\omega - M\alpha)\sin \omega t_n - (\alpha + M\omega)\cos \omega t_n]. \tag{48}$$

The values of t_n are calculated directly from (32):

$$\omega t_n = \tan^{-1}(-1/M) + n\pi, \qquad n = 1, 2, 3, \cdots. \tag{49}$$

To obtain the relationship between two sucessive F_n, the following expressions are derived from (49):

$$\sin \omega t_n = -\sin \omega t_{n-1}$$
$$\cos \omega t_n = -\cos \omega t_{n-1}. \tag{50}$$

Observing (48) and (50), one can see that

$$F_n = -F_{n-1}. \tag{51}$$

Substituting (47) into (46) and using (51) yields

$$I = -E_0 + 2F_1 \sum_{n=1}^{\infty} e^{-\alpha t_n}. \tag{52}$$

According to (49)

$$\alpha t_n = \alpha t_{n-1} + \alpha\pi/\omega. \tag{53}$$

This permits the using of a geometric progression formula on (52), which yields

$$I = -E_0 + \frac{2F_1 e^{-\alpha t_1}}{1 - e^{-\alpha\pi/\omega}}. \tag{54}$$

The trigonometric functions which are required for the calculation of F_1 are obtained from (49):

$$\sin \omega t_1 = 1/\sqrt{1 + M^2}$$
$$\cos \omega t_1 = -M/\sqrt{1 + M^2} \tag{55}$$

Using the last equations, F_1 can be calculated:

$$F_1 = \frac{\omega\sqrt{1 + M^2}}{\alpha^2 + \omega^2}. \tag{56}$$

E_0 is equal to F_0, and obtained by substituting $t = 0$ in (48):

$$E_0 = -\frac{\alpha + M\omega}{\alpha^2 + \omega^2}. \tag{57}$$

To summarize, the integral of the absolute error is given by (54), where E_0, F_1 and t_1 are given in (57), (56), and (49). respectively. For the particular case of a continuous system, the values of α, M and ω are given in (25), (27), and (28). Substituting these values yields

$$I = \frac{2}{\omega_n}\left[\xi + \frac{e^{-M\sigma}}{1 - e^{-M\pi}}\right]. \tag{58}$$

M is given in (27) and $\sigma = \tan^{-1}(-1/M) + \pi$. The minimum value of $(I\omega_n)$ found by computer solution is 1.605, and is obtained for a damping factor of

$$\xi = 0.662.$$

The resulted maximum overshoot is 6.2 percent. As was mentioned above that the square-error criterion prescribes ξ for the continuous case which results an overshoot of 16.3 percent.

The optimal ξ which results a minimum of $(I\omega_n)$, was computed for the sampled-data system. The locus corresponding with the optimal ξ is plotted in Fig. 8.

The values of $I\omega_n$, the damping factor, and the percentage overshoot are almost constant along the optimal locus. In the range $0 < T/\tau < 2$ they vary as follows:

$$2.00 < T/\tau < 0$$

$$0.65 < \xi < 0.66$$

$$6.8 \text{ percent} > \text{percent OS} > 6.2 \text{ percent}$$

$$1.55 < I\omega_n < 1.61.$$

On the other hand, the settling time and the position steady-state error increase with increasing T. The time correspondence to the first overshoot, t_{max}, was calculated from (34). The values of (t_{max}/τ) and the steady-state error as well as the values of $K\tau$ along the locus are given in Table I. The integral of the absolute error (IAE) seems to be the most suitable criterion for servo design and will be used henceforth in the design procedure.

It might be of interest to point out that the IAE criterion takes into account the two contrary design requirements of servo systems, namely small overshoot on the one hand and minimum position error on the other hand. The term E_0 of (54) is the steady-state position error, as can be seen by comparing (41) and (57), and the maximum overshoot, (34), proportional to the term F_1.

Repeating the example of a system in which both the time-constant and the sampling period are 10 ms, and using Fig. 8, an optimal K of 36 s^{-1} is obtained. The maximum overshoot in this case is only 6.5 percent compared with 17.2 percent and 34.3 percent obtained when using the optimal lines of Fig. 6 and Fig. 5, respectively.

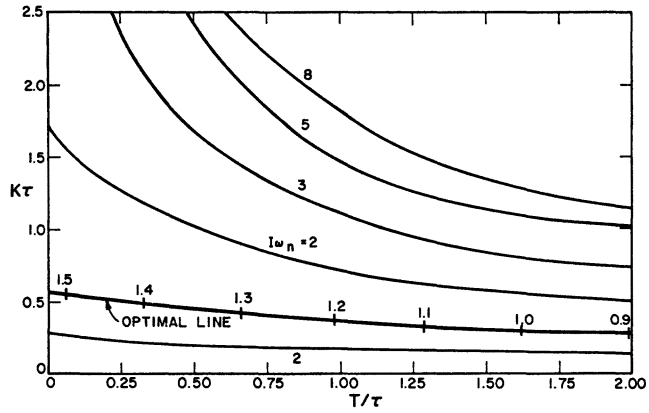

Fig. 8. Loci of integral of absolute error with optimal line corresponding with its optimal ξ, and bandwidth parameter given along line.

TABLE I
DATA ALONG OPTIMAL ABSOLUTE ERROR LOCUS

$\frac{T}{\tau}$	$K\tau$	$\frac{t_{max}}{\tau}$	$\frac{1}{\tau}\int_0^\infty \epsilon dt$	τf_0
0	0.57	5.56	1.75	0.129
0.25	0.50	5.94	1.88	0.119
0.50	0.44	6.35	2.01	0.110
0.75	0.40	6.75	2.13	0.104
1.00	0.36	7.14	2.25	0.097
1.25	0.34	7.55	2.36	0.092
1.50	0.31	7.96	2.47	0.087
1.75	0.29	8.33	2.57	0.083
2.00	0.27	8.71	2.66	0.079

FREQUENCY RESPONSE

The sinusoidal behavior of the system is obtained by substituting $z = e^{st}$ and replacing the Laplace operator s by $j\omega_r$ (ω_r is the circular frequency) in the system transfer function. For the transfer function given by (11), this yields

$$M = \frac{C}{R} = \frac{AP_1 + B + jAS_1}{P_2 + QP_1 + B + E + j(S_2 + QS_1)} \tag{59}$$

where

$$P_1 = \cos \omega_r T;$$

$$P_2 = \cos 2\omega_r T;$$

$$S_1 = \sin \omega_r T;$$

$$S_2 = \sin 2\omega_r T.$$

$$Q = A - 1 - E;$$

(Note that $z = P_1 + jS_1$ and $z^2 = P_2 + jS_2$.)

Equation (59) contains gain and phase information. Usually the main concern is the gain, which is determined by the absolute value of M, given by

$$|M| = \left[\frac{A^2 + B^2 + 2ABP_1}{(B+E)^2 + Q^2 + 1 + 2[(B+E)P_2 + (B+E+1)QP_1]}\right]^{1/2}. \tag{60}$$

Bearing in mind that $B + E + Q + 1 = A + B$, (60) can be rewritten as

$$M = \left[\frac{(A+B)^2 + 2AB(P_1 - 1)}{(A+B)^2 + 2G(P_1 - 1)}\right]^{1/2} \tag{61}$$

where

$$G = (B + E + 1)Q + 2(B + E)(P_1 + 1). \tag{62}$$

The bandwidth is the characteristic of the frequency response which is of most interest. The bandwidth is the frequency range from zero through f_0, where the cutoff frequency f_0 is ordinarily defined as the frequency in which the gain decreases by 3 dB, compared with its dc value. Following this definition, the cutoff frequency is found by equating M to 0.7. Since $P_2 = 2P_1^2 - 1$, a quadratic equation is obtained. The value of (τf_0) was calculated along the minimum absolute-error line, and some results are given in Table I.

Sinusoidally varying inputs are fed into the control loops in a CNC system whenever a circular interpolation is required. The maximum angular velocity depends on the maximum required feed-rate, F_m in in/min, and on the minimum permitable radius of cutting r_m in inches:

$$\omega_m = F_m/60r_m. \tag{63}$$

As limits, consider a typical maximum feed-rate as 60 in/min and a minimum radius of 1 in, which yields $\omega_m = 1$ rad/s. A gain decrease of -3 dB (30 percent error) as the definition of a bandwidth can not be applied in NC controls. When cutting a circle, the error e_r in the radius r is not allowed to exceed one-half of the resolution in the entire range from dc through ω_m. The bandwidth of the system depends on the maximum relative error (e_r/r). For example, if the resolution of the system is 10^{-4} in, the maximum relative error, for a minimum cutting radius of 1 in is

$$\frac{e_r}{r} = 5.10^{-5}. \tag{64}$$

When cutting along a circle with larger radius, ω_m decreases causing the produced error e_r to decrease with $\omega_m{}^2$, as will be shown later. On the other hand, a circle with a radius smaller than 1 in is produced with reduced feedrates and, in addition, the permitted relative error (e_r/r) is allowed to be greater than 0.00005. Therefore, the requirement prescribed by (64) is realistic for NC applications.

The contour errors in circular cutting in the continuous case were investigated in [10] for various values of ξ. It has been shown in [10] that the steady-state relative error in the radius is

$$\frac{e_r}{r} = 1 - |M| \tag{65}$$

By substituting (61) into (65), the relationship between ω_r and (e_r/r) is obtained. For very small error, ω_r is also small, and the following approximations are allowed:

$$P_1 + 1 \cong 2$$

$$M^2 \cong 1 - 2(e_r/r).$$

This yields the equation

$$(AB - G)(1 - P_1) = (A + B)^2 e_r/r. \tag{66}$$

By substituting the values of A, B, and G into (66), one obtains

$$\frac{e_r}{r} = \frac{L}{T^2}(1 - P_1) \tag{67}$$

where

$$L = \frac{K(T + 2\tau) - 1}{K^2}. \tag{68}$$

By substituting (64) into (67), the maximum permitted ω_r, denoted as ω_{rm}, is obtained as a function of K, T, and τ. Some results of $[100 \cdot \tau\omega_{rm}]$ are summarized in Table II and are also given as a parameter along the optimal line of the absolute-error in Fig. 8. Obviously, the system designs must meet the requirement

$$\omega_m < \omega_{rm}. \tag{69}$$

Using a further approximation of $P_1 \cong 1 - (\omega_r T)^2/2$, (67) is reduced to

$$\frac{e_r}{r} = \frac{L}{2}\omega_r{}^2, \tag{70}$$

showing the parabolic relationship between the error and ω_r for small errors.

The main result of this section is (67), which by substituting (64) and (68) gives the useful bandwidth for sinusoidal inputs. The 3-dB bandwidth f_0, which was calculated at the outset, is useful as a number to characterize the disturbance rejection ratio, especially when the axis is not in motion but is subjected to torque disturbances due to the cutting action of the other axes.

DESIGN PROCEDURE

The position loop gain can be determined by using a formula recommended by [11, pp. 5-4]

$$K = \frac{1}{50\tau_0}\left[\frac{\text{units/min}}{\text{milliunits}}\right] \tag{71}$$

where τ_0 is the naked system time constant in seconds. In a dimensionless format, (71) is written as

$$K\tau_0 = 1/3 \quad \text{[dimensionless]}. \tag{72}$$

Assuming that the time constant of a loaded system is about 1.5 to 2 times greater than the one of a naked system, we see that the recommendation is a system design with $K\tau$ between 0.5 ($\xi = 0.71$) to 0.67 ($\xi = 0.61$). Using the IAE criterion, prescribes $K\tau = 0.57$ for a continuous system, which is within the recommended range.

When the same system is applied to CNC, the new parameter T must be chosen. The minimum value of T depends on

TABLE II
BANDWIDTH ALONG OPTIMAL CURVE

T/τ	$K\tau$	$100\tau\omega_{rm}$
0	0.567	1.52
0.25	0.499	1.42
0.42	0.460	1.37
0.50	0.443	1.35
0.75	0.400	1.26
0.90	0.378	1.22
1.00	0.365	1.18
1.25	0.336	1.11
1.50	0.312	1.03
1.63	0.300	1.00
1.75	0.291	0.96
2.00	0.274	0.89

the processing time of the CNC program; the maximum value depends on the required bandwidth. Let us define the bandwidth parameter of Table II by B, i.e.,

$$B = 100\tau\omega_{rm}. \tag{73}$$

Table II was derived for a minimum radius of 1 in. Using the data in (63) provides the relationship between the bandwidth and the maximum feed-rate in in/min:

$$\tau F_m = 0.6B \tag{74}$$

where τ is in seconds. Since τ and F_m are known, B can be determined. T/τ is found either by using the calibration along the optimal line in Fig. 8, or with the aid of Table II.

For example, for $F_m = 60$ in/min and $\tau = 10$ ms, the value of B, as derived from (74), is 1. The corresponding value of T/τ, as found from Table II, is 1.63, which means that $T = 16.3$ ms, or a minimum sampling frequency of 61 Hz. Assuming that a sampling period of 15 ms was chosen for this system, the optimal gain, as determined from Table II, is

$$K_0 = \frac{0.312}{\tau} = 31.2\ \mathrm{s}^{-1} = 1.87\left[\frac{\text{in/min}}{\text{mil}}\right]. \tag{75}$$

The corresponding time response is given in Fig. 9(a)[1]; the calculated overshoot is 6.7 percent. Notice that the value of τ prescribes a limit on F_m. In the continuous case, the limit, as derived from (74) and Table II, is

$$\tau F_m = 0.91. \tag{76}$$

In the sampled-data case, the minimum value of T must be used to determine this limit.

Since the relationship between K and T has been originally derived here, let us assume that the designer wishes to meet the requirement of a continuous system, i.e., $K\tau$ ranges between 0.5 to 0.67. In order to overcome the sampling influence, the designer will probably choose the smaller value of 0.5, which yields a K of 50 s^{-1}. The corresponding time response is given in Fig. 9(b), and the calculated overshoot is 23 percent. Notice that according to [11], "Overshoot of over 20 percent could result in unsatisfactory servo performance." The ratio between 23 percent and 6.7 percent does not depend on the value of τ. For example, for $\tau = 20$ ms and $F_m = 30$ in/min, the optimal gain is 15.6 s^{-1} as derived from the requirement $K\tau = 0.5$, yielding the ratio of 6.7/23 in the overshoot.

[1] The control computer is SDS 930 of the DASL Laboratory.

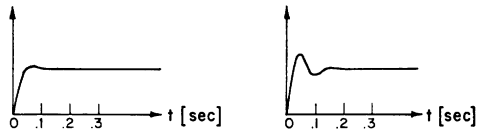

(a) (b)

Fig. 9. Time response of sampled-data system with 15-ms sampling period and 10-ms time constant. (a) $K_\tau = 0.3$. (b) $K_\tau = 0.5$.

CONCLUSIONS

A sampled-data control loop for CNC machine tools has been analyzed, and the relation between the loop gain and the computer sampling rate has been derived. Different criteria were investigated in order to find the optimum performance. The integral of the absolute error has been chosen as the most useful approach, and its optimal curve was calculated. In order to find the optimal point on this curve, the relationship between the maximum feedrate in circular interpolation and the sampling period was inferred from the system bandwidth. This provides the control engineer with a systematic design procedure for the selection of system parameters.

REFERENCES

[1] A. Poo and J. G. Bollinger, "Digital-analog servo system design for CNC," 9th Annual Meeting of the IEEE Ind. Appl. Society, Paper IC-WED-AM3, Oct. 1974, pp. 621-623.
[2] Y. Koren, A. Shani, and J. Ben-Uri, "Overshoot correction in digital control system," *Control*, vol. 13, no. 129, pp. 204-205, Mar. 1969.
[3] Y. Koren, A. Shani, and J. Ben-Uri, "Overshoot correction in digital control of a lathe," *IEEE Ind. Gen. Appl.*, vol. 6, no. 2, pp. 175-179, Mar. 1970.
[4] J. R. Ragazzini and G. F. Franklin, *Sampled-Data Control Systems.*" New York: McGraw-Hill, 1958.
[5] E. I. Jury, *Sampled-Data Control Systems.* New York: Wiley, 1958.
[6] J. T. Tou, *Digital and Sampled-Data Control Systems.* New York: McGraw-Hill, 1959.
[7] B. C. Kuo, *Analysis and Synthesis of Sampled-Data Control Systems.* Englewood Cliffs, NJ: Prentice, 1963.
[8] E. G. Gilberg, "Dynamic error analysis of digital and combined analog digital computer systems," *Simulation*, vol. 6, pp. 241-257, Apr. 1966.
[9] G. J. G. Turxal, *Automatic Feedback Control System Synthesis.* Tokyo: McGraw-Hill (Kogakusha Co.) 1955, p. 523.
[10] A. N. Poo and J. G. Bollinger, "Dynamic errors in type 1 contouring systems." *IEEE Trans. Ind. Appl.*, vol. IA-8, no. 4, July/August 1972, pp. 477-484.
[11] General Electric, "Pulse width modulated servo drive," GEK-36203, Mar. 1973.

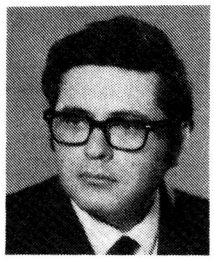

Yoram Koren (M'76) received the B.Sc., M.Sc., and D.Sc. degrees, all in electrical engineering, from the Technion-Israel Institute of Technology, Haifa, Israel in 1965, 1968, and 1971, respectively.

In 1967 he was employed as a Research Engineer by Elbit Control Inc., Haifa. From 1971 through 1973, he was a Lecturer at the Technion and at the Ben-Gurion University in Beer-Sheva. He later supervised the development of the computer numerical control milling machine project at McMaster University, Metal-Working Research Group, Hamilton, ON, Canada. In 1974, he joined the staff of the Engineering Experiment Station, University of Wisconsin-Madison, and conducted research on computer control and data acquisition. In 1975 Dr. Koren returned to the Technion-Israel Institute of Technology, where he is now Senior Lecturer in the Material Processing and Machine Tool Center, Faculty of Mechanical Engineering, teaching and conducting research in computer control and automation of machine tools.

John G. Bollinger received the B.S. degree from the University of Wisconsin, Madison, the M.S. degree from Cornell University, Ithaca, N.Y., and the Ph.D. degree from the University of Wisconsin.

His industrial experience includes research and development work in the aircraft, electronics, and machine tool industries through summer employment. At present he is a Professor in the Department of Mechanical Engineering, University of Wisconsin. Over the past several years, he has been responsible for teaching and research in mechanical design, including lecturing in vibrations, automatic controls, noise analysis and control, and fundamental design. In the field of controls education he is the coauthor of *Introduction to Automatic Controls.* He is concerned with control problems in the machine tool, paper, and steel fabricating fields. As an industrial consultant, he deals with special technical problems and the presentation of in-plant courses and seminars. Most recently, he has been involved in the fields of digital computer control and environmental noise control.

Basic Operating Characteristics of a High-Frequency Inverter with Capacitive Voltage Multiplier

NICOLAE D. LUDU

Abstract—**The integrodifferential equations of the equivalent circuit are solved, and the operating characteristics are derived for a current-fed thyristor inverter. This inverter can be especially useful as a high-frequency power source for induction heating.**

INTRODUCTION

THE MODERN induction heating and melting plants are equipped with solid state high-frequency SCR inverters. These static inverters have several advantages over the classical motor-generator sets, such as higher efficiency, small space and weight, simpler installation, quieter operation, and no maintenance.

A good number of high-frequency inverters have been already treated in literature [1]-[11]. Thus the voltage-fed inverter is discussed in [7], [8] and the current-fed inverter is discussed in [3] and [5]. A comparative examination between voltage-fed and current-fed inverters is presented in [4] and [10]. Some features of the inverter with capacitive voltage multiplier are disclosed in [6]. This is a current-fed inverter which can operate under load-voltage amplitude greater than thyristor-voltage amplitude.

Paper approved by the Static Power Converter Committee of the IEEE Industry Applications Society for publication in this TRANSACTIONS. Manuscript released for publication March 30, 1977.

The author is with the Department of Switchgears and Converters, Bucharest Polytechnic Institute, Romania.

The original contribution of the present paper is to perform a steady-state analysis of the current-fed inverter with capacitive voltage multiplier and to derive its basic operating characteristics. The results obtained are presented both analytically and graphically as a function of load and output frequency changes. These results permit a deeper understanding of the inverter behavior and can be used by the designer to select the optimum circuit components.

Tests were carried out by means of a laboratory inverter in order to experimentally verify the operating characteristics.

I. BASIC INVERTER CONFIGURATION AND EQUIVALENT CIRCUIT

The basic schematic of the current-fed bridge inverter with capacitive voltage multiplier is shown in Fig. 1. The load is represented by the equivalent load resistance R and the equivalent load inductance L. As compared to the basic current-fed inverter [3], the inverter shown in Fig. 1 includes a capacitor C_1 connected in series only with the load $R - L$. As will be seen, the capacitors C and C_1 operate as a capacitive voltage multiplier. This means that the peak value of e_L (see Fig. 1) will be larger than the peak value of e, and accordingly, the SCR blocking capability could be more conveniently used. For larger load voltages, this major advantage of the current-fed inverter with capacitive voltage multiplier over the basic current-fed inverter permits the avoiding of SCR series techniques.

0093-9994/78/0300-0264$00.75